DESIGN AND EXPERIMENTAL STUDY OF A SELF-PROPELLED ELECTRIC TRACKED CHASSIS FOR *PANAX NOTOGINSENG* TRANSPLANTER IN HILLY AND MOUNTAINOUS REGIONS

/

丘陵山区自走式三七移栽机电动履带底盘设计与试验研究

Wei SU[1)], Congcong LIAO[1)], Qingxu YU[*2)], Yi ZENG[1)], Qinghui LAI[1)], Cantong SU[1)]
[1)]University of Science and Technology Kunming, Kunming 650093, China;
[2)]Nanjing Institute of Agricultural Mechanization, Ministry of Agriculture and Rural Affairs, Nanjing 210014, China;
** Correspondent authors: Qingxu YU; E-mail: yqx5205@163.com*
DOI: https://doi.org/10.35633/inmateh-79-41

Keywords: *Panax notoginseng transplanter; fully electric intelligent tracked chassis; speed-measuring encoder; speed-synchronized cooperative transplanting control; hilly and mountainous regions; straight-line deviation correction control*

ABSTRACT

To address the challenges of low transplanting efficiency, poor planting accuracy, and high labor intensity associated with manual Panax notoginseng transplanting in the hilly and mountainous regions of Yunnan, as well as the limited adaptability of existing transplanting equipment to narrow ridged fields and steep, complex terrain, this study developed a self-propelled, fully electric tracked chassis tailored to the agronomic requirements of Panax notoginseng transplanting. The study included the overall structural design, selection and matching of the power battery and drive transmission system, and development of a dimensionless ratio-coefficient control model relating planting spacing to travel and transplanting speeds under the constraint of the manual seedling-feeding speed. An integrated electronic control system was developed to provide remote-controlled travel, speed-synchronized transplanting control, and straight-line deviation correction. The stability and dynamic performance of the chassis were analyzed theoretically and subsequently validated through field tests under multiple operating conditions. Theoretical results showed that the chassis had a maximum lateral roll angle of 39.19°, a maximum traction force of 7,524 N, and sufficient power reserve for operation on slopes of up to 25°. Field tests demonstrated that, after correction using the speed-adjustment coefficient, the straight-line deviation over a travel distance of 30 m was limited to within 1.1%, exceeding the requirements of the relevant national standard. The measured pivot-turning offset was approximately 191 mm, in close agreement with the theoretical value. Key performance indicators, including slope-climbing stability, ridge-travel stability, and motor thermal stability, all met the applicable national standards. The developed chassis effectively improves the adaptability of transplanting equipment for Panax notoginseng production in hilly and mountainous regions and significantly enhances the automation level and planting accuracy of transplanting operations. This study provides theoretical and technical support for the intelligent development of transplanting equipment for rhizomatous medicinal plants.

摘要

针对云南丘陵山区三七人工移栽效率低、栽植精度差、劳动强度大，且现有移栽装备难以适配垄上窄幅作业与陡坡复杂地形的产业痛点，本文设计一款适配三七移栽农艺需求的丘陵山区自走式纯电动履带底盘。完成整机结构方案设计、动力电池与驱动传动系统的选型匹配，基于人工投苗速度极限建立株距与行走-移苗速度的无量纲配比系数调控模型，开发集遥控行走控制、随速协同移栽控制、直线度纠偏控制于一体的电控系统，并开展整机稳定性与动力性能的理论计算，以及多工况田间性能验证试验。理论计算结果表明：该底盘横向极限倾翻角达 39.19°，最大牵引力 7524 N，动力储备满足 25°陡坡作业；田间试验结果显示：经速度修正系数纠偏后，整机 30 m 行程直线度误差可控制小于 1.1%，优于国家标准限值；原地转向中心偏移量实测约 191 mm，符合理论计算值；爬坡稳定性、垄上行驶稳定性及电机热稳定性等核心性能指标均满足相关国标要求。该底盘有效解决丘陵山区三七移栽的装备适配难题，显著提升移栽作业的自动化水平与栽植精度，可为根茎类中药材移栽装备的智能化升级提供理论与技术支撑。

---

[1] *Wei SU, Ph. D. Professor; Qingxu YU, Ph. D. Assistant Researcher; Qinghui LAI, Ph. D. Professor; Congcong LIAO, Master Candidate; Yizeng ZENG, Master Candidate; Cantong SU, Master Candidate.*

INTRODUCTION

To address the practical challenges associated with manual transplanting of *Panax notoginseng* in the hilly and mountainous regions of Yunnan—including low efficiency, poor planting accuracy, and high labor intensity—as well as the limited adaptability of existing transplanting equipment to narrow ridges and steep, complex terrain *(Liu et al., 2025; Zhang, 2025; Zhu, 2025)*, an electric direct-drive, remote-controlled chassis is needed. The chassis should provide rapid dynamic response, stable operation *(Xu et al., 2023)*, and reliable remote-control capability, enabling it to operate effectively under narrow-width field conditions. By coordinating travel speed with the seedling-transplanting speed, the system can maintain accurate planting spacing and meet the operational requirements of ridged *Panax notoginseng* transplanting.

In the field of tracked chassis research, scholars worldwide have conducted extensive investigations, providing a solid theoretical and technical foundation for performance optimization. International studies have primarily focused on three directions: stability control, motion resistance analysis, and design evaluation versatility. *Rocha et al., (2023),* proposed an attitude controller integrating dual quaternions with the differential kinematics of a Stewart platform, enabling active track flap adjustments for terrain adaptation on rough ground. *Shafaei* & *Mousazadeh, (2023),* investigated the resistance characteristics of rubber track landing gears for autonomous towed robots, clarifying the effects of speed and load on resistance and suggesting optimization directions. *Dobretsov et al., (2021),* introduced a deterministic calculation method based on the Bernstein–Letoshnev relationship to effectively assess chassis–soil mechanical parameters. Validation using an eight-ton chassis demonstrated that this method outperforms stochastic approaches.

Chinese researchers have proposed various optimization strategies to address common challenges in the autonomous navigation and motion control of tracked chassis *(Liu et al., 2025; Zhao et al., 2024)*. *Qi et al., 2024,* developed a three-tangent path planning algorithm to mitigate the control deficiencies of single-side braking steering in tracked chassis, significantly improving path tracking stability and reducing steering control frequency. In response to the operational demands of complex environments such as hilly and mountainous regions and orchards, Chinese researchers have conducted targeted design and development efforts focusing on critical performance indicators, including trafficability and stability *(Chen et al., 2025; Zhang et al., 2025; Li et al., 2025; Wang et al., 2025)*. *Nie Jianjun et al., (2025),* designed an arch-shaped agricultural robot chassis with an adjustable posture tailored for hilly terrains, verifying its superior terrain adaptability and travel performance.

Addressing specific planting patterns and operational requirements, domestic researchers have also developed specialized chassis and their control systems *(Hao et al., 2024; Zhu et al., 2023)*. *Yu et al., (2025)*, tackling the challenges in rhizome transplanting of medicinal materials, designed an electronic control system for transplanters based on STM32 and fuzzy PID, validating its superior performance over traditional PID schemes, thereby providing theoretical and technical support for the mechanization of medicinal material transplanting. Additionally, some scholars have conducted foundational research on chassis performance prediction and validation, offering critical support for design optimization *(Liu et al., 2025)*. *Zhang et al., 2023*, addressing the performance deficiencies of a *Panax notoginseng* combined harvester chassis, investigated chassis trafficability under heavy clay soil conditions, providing theoretical references for the design of rhizomatous crop harvester chassis in hilly and mountainous regions.

In summary, the application of fully electric tracked chassis in the transplanting of rhizomatous medicinal materials remains underexplored. To address this gap, this study proposes a fully electric tracked chassis specifically designed for *Panax notoginseng* transplanting, integrating the characteristics of ridged planting and the steep terrain typical of hilly and mountainous regions. The chassis is tailored to the operational requirements of *Panax notoginseng* transplanting, with a core focus on the demanding conditions of low-speed, high-load operation. This capability to accommodate low travel speeds under substantial load during transplanting constitutes a key advantage distinguishing it from general-purpose chassis. To validate its performance under such conditions, a series of tests were conducted, including speed measurement, straight-line deviation correction, and pivot turning offset evaluation. Furthermore, a speed-synchronized control system was developed to precisely measure the travel speed of the transplanter. Using this measured speed as the target, a PID control algorithm was employed to regulate the seedling conveying belt motor, enabling coordinated control between the seedling conveying belt and travel motors, ultimately achieving precise transplanting.

MATERIALS AND METHODS

Test materials

The design, fabrication, and assembly of the chassis system and core working components of the *Panax notoginseng* transplanter developed in this study were completed by Sanniu Agricultural Machinery Manufacturing Co., Ltd. in Dingxi City, Gansu Province. After preliminary debugging and performance baseline tests of the prototype were conducted at the company's experimental field, comprehensive performance validation tests were carried out on January 19, 2026, at the Engineering Training Center of Kunming University of Science and Technology to fully verify the operational stability of the whole machine and optimize key working parameters.

Test equipment

All measuring instruments used in these tests were calibrated, with accuracy meeting the relevant requirements of the test specifications. Environmental parameter collection and measurement were strictly conducted in accordance with GB/T 5262—2008, "General Rules for Measuring Methods of Agricultural Machinery Test Conditions" *(General Administration of Quality Supervision, Inspection and Quarantine of P.R.China & Standardization Administration of P.R.China, 2008)*. The data obtained provide a reliable foundation for subsequent analysis of operational performance and optimization of key parameters.

Machine structure and working principle

Given the complex terrain of Yunnan's hilly and mountainous regions and the specific transplanting mode under *Panax notoginseng* shade shelters, the structural parameters of the tracked self-propelled transplanter chassis significantly affect critical performance metrics such as passability on sloping terrain *(Han et al., 2022)*. Through specialized chassis design, this study achieves a marked improvement in the trafficability of irregular pathways between planting ridges.

Table 1

Design Parameters of the Tracked Chassis

Parameters	Value	Parameters	Value
Overall length/mm	1400	Effective drive-wheel diameter/mm	150
Overall width/mm	1360	Total mass/kg	780
Overall height/mm	1050	Minimum ground clearance/mm	350
Track width/mm	230	Inner distance between tracks/mm	900
Idler wheel diameter/mm	150	Ground contact length/mm	850
Guide wheel diameter/mm	200	Maximum climbing angle/(°)	≥25

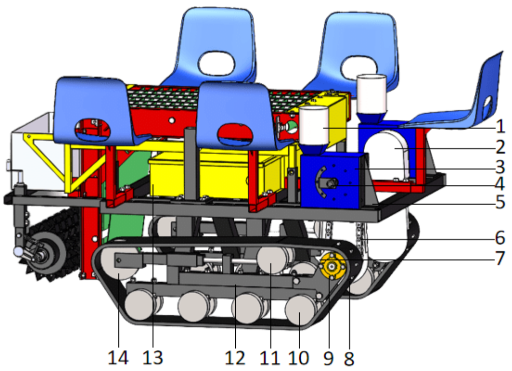

Fig. 1 - Schematic of the tracked chassis of the *Panax notoginseng* transplanter
1. Motor; 2. Chain guard; 3. NMRV110 gearbox; 4. Encoder; 5. Gearbox mounting plate; 6. Drive chain; 7. Track drive sprocket; 8. Track 9. FC207 bearing housing; 10. Idler wheel; 11. Drive wheel; 12. Chassis; 13. Battery box; 14. Guide wheel

The structure of the tracked chassis for the *Panax notoginseng* transplanter is illustrated in Figure 1. The machine employs a brushless DC motor coupled with an NMRV110 reducer, driving the tracked traveling mechanism via chain transmission. The power transmission path follows the sequence: motor, reducer, output shaft, sprocket and chain, drive wheel, and tracks, with assistance from supporting rollers and guide wheels to enable movement.

Given the operational demands of steep slopes in hilly regions, the electric chassis is required to achieve a climbing capability of no less than 25° and must not tip over when traversing laterally on slopes. The frame adopts a 1360 mm wide-base design with a low-center-of-gravity layout. Combined with the independent support on both sides of the tracks and the large ground contact area, this configuration significantly enhances anti-overturning capability and operational stability on complex slopes *(Mo, 2025; Mu et al., 2024; Quan & Ma, 2010)*.

Design and Selection of Key Chassis Components

To address the power requirements, agronomic compatibility, and intelligent control objectives for *Panax notoginseng* transplanting operations in the hilly and mountainous regions of Yunnan, this chapter focuses on the core working systems of the chassis. It presents the specialized design, parameter selection, and performance matching of the power battery system, drive motor system, and control system. These efforts ensure stable power output, precise coordination between travel and seedling transplanting operations, and flexible and reliable field maneuverability, thereby fully meeting the demands of narrow ridged field operations and steep, complex terrains.

Design and Selection of the Power Battery System

To meet the continuous operation and operational stability requirements of the traveling, transplanting, and electronic control systems of the *Panax notoginseng* transplanter, a dual-power supply architecture is adopted. The traveling power circuit is powered by a high-capacity battery pack consisting of sixteen 12 V/65 Ah lead-acid batteries configured in series-parallel to provide 48 V/260 Ah. The seedling transplanting power circuit is powered by a dedicated battery pack composed of two 12 V/20 Ah lead-acid batteries connected in series to supply 24 V/20 Ah, providing exclusive power to the seedling transplanting actuator. The control circuit employs an independent lithium battery module to deliver a stable 5 V power supply to controllers, sensors, and other components, achieving isolation between high-voltage and low-voltage electrical systems, thereby ensuring control accuracy and signal transmission stability. Under a rated operating voltage of 48 V supplied by the 260 Ah battery pack, the chassis operates in the field at full power of 4.4 kW. The endurance time of the traveling system is calculated using the following formula:

$$T=\frac{CkU}{P} \tag{1}$$

where: C — capacity of lead-acid battery pack (260 Ah)

U — rated voltage of travel motor (48 V)

P — actual power of travel motor (4400 W)

k — actual usable capacity factor of lead-acid batteries (0.8)

According to calculation, the full-power field operation duration of the chassis is approximately 2.3 hours.

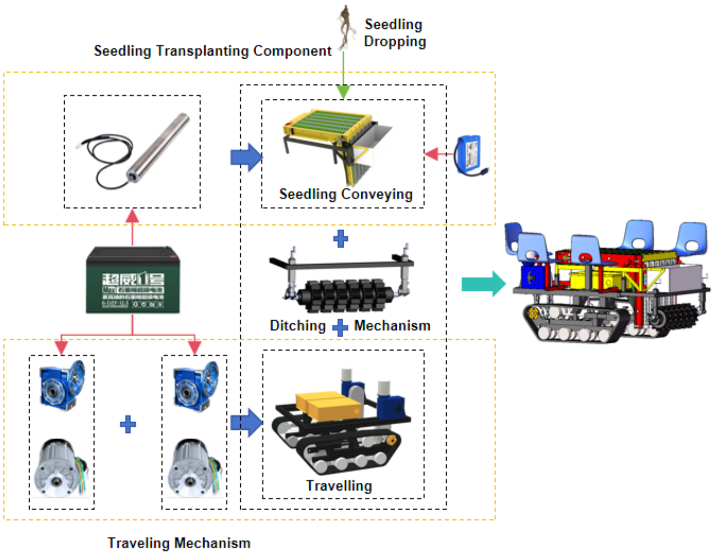

Fig. 2 - Schematic diagram of the power supply system for a transplanter

Design of the Drive Motor and Transmission System

The drive motor system serves as the power core for the chassis traveling and transplanting operations. Its parameter selection, transmission system matching, and coordinated design of operating speed directly determine the traction performance, climbing capability, and transplanting spacing accuracy of the whole machine.

Based on the agronomic requirements of *Panax notoginseng* transplanting and the limits of manual seedling feeding speed, this study completes the selection and design of the drive motor and transmission components, establishes a coordinated matching model for traveling and seedling transplanting speeds, thereby ensuring both dynamic performance and operational precision.

Coordinated Matching Model of Traveling and Seedling Transplanting Speeds under Manual Feeding Constraint

The transplanting operation of *Panax notoginseng* adopts a manual seedling feeding method, where the feeding rate serves as a critical constraint affecting the overall operating speed, seedling conveyor belt speed, and planting spacing. Experimental results indicate that the upper limit of manual feeding rate per person is 0.5 plants/s, with the machine employing four operators working simultaneously. Based on this constraint, a dimensionless ratio coefficient regulation model correlating planting spacing with traveling and seedling transplanting speeds was established, as illustrated in Figure 3.

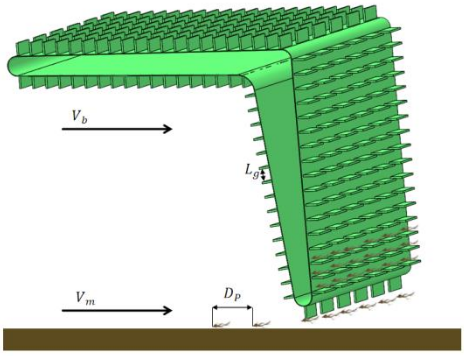

Fig. 3 - Schematic of seedling transplanting

The transplanting spacing is defined as the linear distance traveled by the transplanter along its direction of travel during the interval between the moment a preceding seedling drops into the planting soil and the moment the next seedling reaches the exit of the seedling conveyor belt. The underlying principle is illustrated in Figure 3.

The time interval for the subsequent seedling to reach the exit of the seedling conveyor belt can be expressed as $t=L_g/V_b$. Based on the physical definition of planting spacing D_p, the calculation formula for planting spacing can be derived as follows:

$$D_p=V_m t=V_m\frac{L_g}{V_b} \tag{2}$$

Introducing the dimensionless ratio coefficient $K=V_m/V_b$, which relates the traveling speed of the transplanter to the seedling conveyor belt speed, and substituting it into the above formula, the theoretical relationship between planting spacing and the ratio coefficient can be simplified as follows:

$$D_p=KL_g \tag{3}$$

where:

D_p— planting spacing (mm)

t — time interval for the next seedling to reach the outlet (min)

V_m — travel speed of transplanter (m/min)

V_b — conveying speed of seedling belt (m/min)

L_g — spacing between partition baffles on seedling conveyor belt (40 mm)

K — dimensionless matching coefficient between transplanter travel speed and seedling belt conveying speed (dimensionless)

To achieve convenient and precise regulation of *Panax notoginseng* transplanting spacing, the dimensionless ratio coefficient K is adopted as the core control parameter, addressing the limitations of traditional dual-speed synchronization methods. Based on the agronomic spacing requirement of Dp=80～200 mm for *Panax notoginseng* and the partition plate spacing Lg=40 mm on the seedling conveyor belt, the reasonable range of $K$is derived as 2～5, enabling precise matching of the corresponding planting spacing requirements.

In the control system, the operator only needs to set the target Kvalue, and the system automatically matches V_m and V_b to achieve single-parameter online regulation of planting spacing.

This approach simplifies operation, ensures regulation accuracy, and enhances equipment adaptability while precisely aligning with the limits of manual seedling feeding, thereby establishing an accurate correlation between operating speed and planting spacing.

Based on the limit of manual seedling feeding speed, the maximum allowable speed of the seedling conveyor belt is derived. Let the operation time be t, then the displacement of the seedling conveyor belt during time t is given by:

$$S_b=V_b t \tag{4}$$

Combined with the planting spacing D_p, the total number of seedlings planted within time t can be calculated as:

$$N=6\times\frac{S_b}{D_p} \tag{5}$$

Given that the maximum manual seedling feeding rate per person is 0.5 plants/s, equivalent to 30 plants/min, the number of seedlings fed per person within t minutes is less than 30t, i.e., $N_S<4\times 30t$. Substituting $S_b=V_b t$ into the inequality and simplifying yields:

$$V_b<\frac{30\times 4D_p}{6}=20D_p \tag{6}$$

where:

N_s — total maximum fry output of four seedling distributors within a fixed time period (plant)

S_b — moving distance of seedling conveyor belt within a fixed time period (m)

t — operation assignment time (min)

6 — coefficient for simultaneous six-row transplanting (dimensionless)

4 — coefficient corresponding to four seedling planting units (dimensionless)

Based on the *Panax notoginseng* transplanting spacing control range of D_p=0.08～0.2 m, the constraint conditions for the seedling conveyor belt speed are derived as follows: when D_p=0.08 m, Vb<1.6 m/min; when D_p=0.2 m, V_b<4 m/min. These constraints ensure that the seedling conveyor belt speed matches the maximum manual seedling feeding rate, preventing missed placements or misalignment caused by excessive belt speed.

Combined with the previously derived formula for planting spacing $D_p=V_m L_g/V_b$, the calculation formula for the transplanter traveling speed can be rearranged to obtain:

$$V_m=\frac{D_p V_b}{L_g} \tag{7}$$

Under the constraint of the maximum manual seedling feeding rate, combined with the limit values of the seedling conveyor belt speed and the planting spacing range, the maximum traveling speed of the transplanter can be calculated as follows: when the planting spacing D_p=0.08 m, the maximum traveling speed is 3.2 m/min; when D_p=0.2 m, the maximum traveling speed is 20 m/min. The traveling speed of the transplanter must match the manual seedling feeding limit. In practical operation, a speed range of 3.2 m/min to 20m/min is recommended to accommodate the planting spacing requirement of 80 mm to 200 mm, ensuring coordinated matching among traveling speed, seedling feeding, and seedling conveying speed.

Matching Calculation of the Transmission Ratio for the Traveling System

Based on the design requirement of adopting the recommended speed range of 3.2~20 m/min in actual operation, and considering factors such as ground slip during tracked field operation and elastic slip in the chain transmission, sufficient margin is reserved for the theoretical traveling speed. Consequently, 22 m/min is ultimately determined as the theoretical maximum reference speed for the matching calculation of the sprocket-chain transmission ratio. The calculation formula for the straight-line traveling speed of the whole machine is:

$$V_m=\frac{\pi n_0 D(1-\delta)}{i_1 i_2} \tag{8}$$

where: V_m — theoretical maximum reference speed (22 m/min)

n_0 — rated speed of brushless DC motor (3000 r/min)

D — effective diameter of track driving wheel (0.15 m)

i_1 — reduction gear ratio (60)

i_2 — gear-chain transmission ratio (dimensionless)

δ— total slip coefficient of transmission system, including chain elastic slip and track-ground slip (0.26)

The calculated transmission ratio i_2≈0.79. Accordingly, the number of teeth on the driving sprocket of the reducer output shaft was selected as 15, and the number of teeth on the driven sprocket of the track drive wheel was selected as 19. This parameter matching scheme enables precise adaptation between the machine's traveling speed, the rated motor speed, and each stage of the transmission system, thereby effectively ensuring traveling stability and synchronization with seedling transplanting during field operations.

Control System Design

To ensure operational flexibility, accurate straight-line travel, and coordinated travel–transplanting performance during field operation of the *Panax notoginseng* transplanter, an electronic control system was developed that integrates remote travel control, speed-synchronized transplanting control, and straight-line deviation correction. The system enables remote control of chassis travel, steering, and emergency stopping, as well as real-time closed-loop coordination between seedling-conveying speed and travel speed. These functions improve the level of operational intelligence and enhance transplanting-spacing accuracy.

The control logic of the remote-control system for the tracked chassis is illustrated in Figure 4. Upon power-up, the system first initializes, followed by communication link verification of the wireless remote-control module, with the verification result indicated via an indicator light: if the module is not successfully connected, the light remains constantly on without flashing; if the connection is normal, the light flashes continuously, and the system enters the command-ready state. The remote controller issues three types of commands: travel commands control the chassis forward/backward movement, steering, and emergency stop; mode switching commands enable switching of operation modes such as cruise control; and motor correction coefficient commands adjust the track motor deviation correction parameters. After executing a command, the system verifies the completion status in real time; if incomplete, the command continues to execute, and upon completion, the control process terminates.

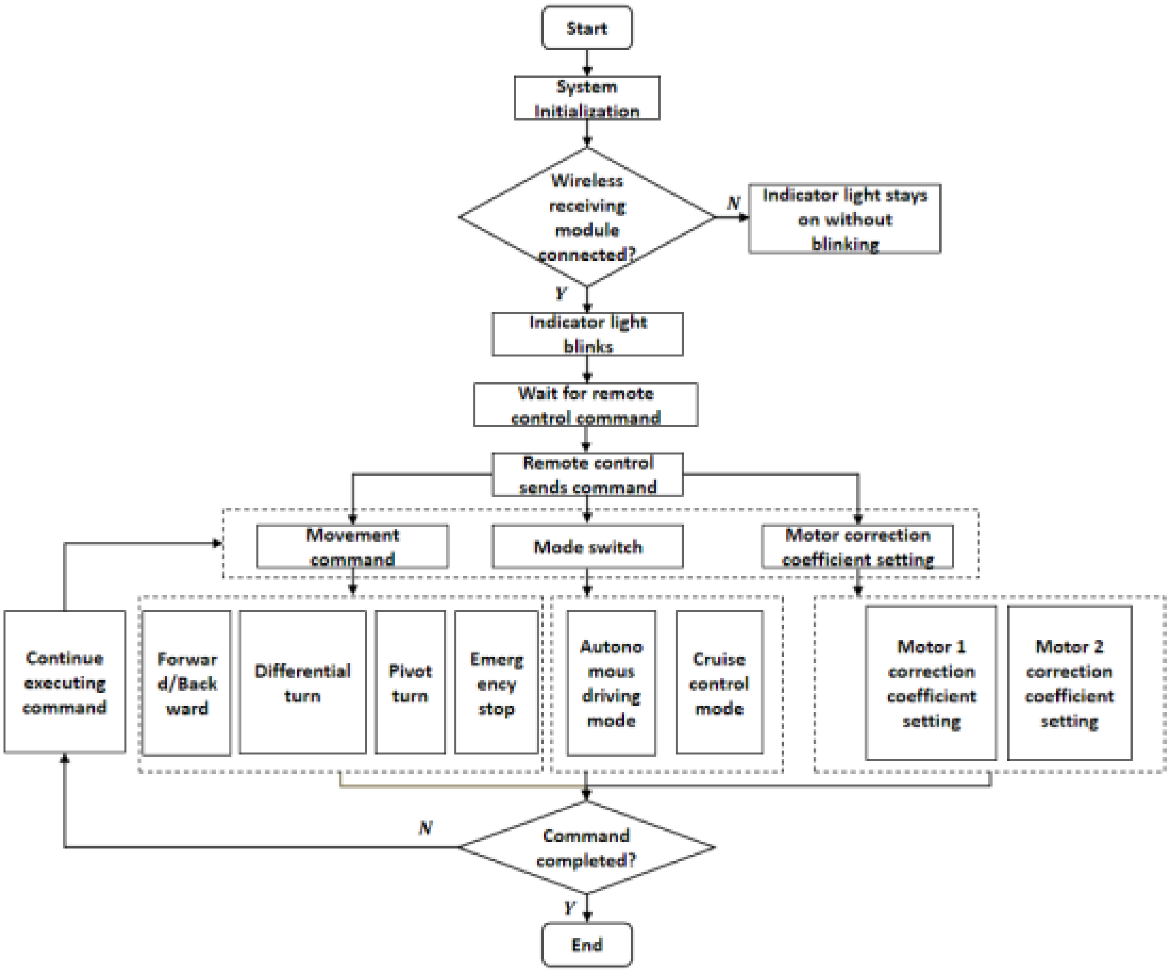

Fig. 4 - Control logic diagram of the remote control system

The speed-synchronized control system designed in this paper operates according to a three-stage architecture of "signal acquisition – main control processing-execution drive," with the core function of achieving real-time coordinated control between the seedling conveyor belt speed and the chassis traveling speed, thereby ensuring the stability and consistency of transplanting spacing. The schematic diagram of the control system is shown in Figure 5.

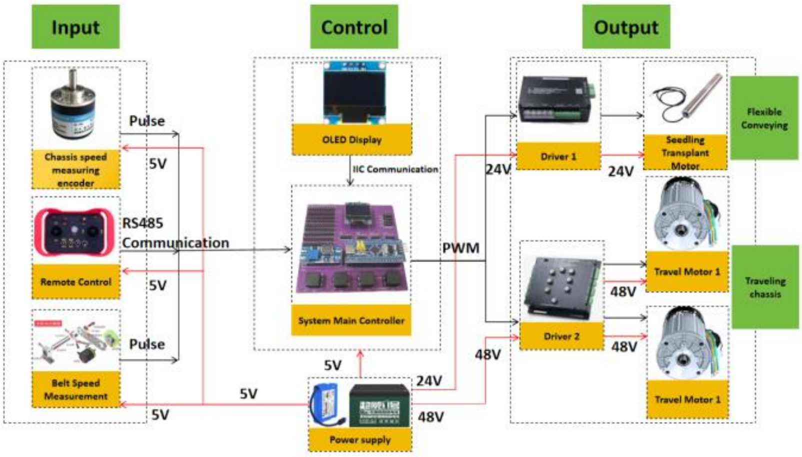

Fig. 5 - Schematic of the control system

During the signal acquisition stage, the chassis speed-measuring encoder and belt speed-measuring encoder at the input end collect pulse signals from one side of the traveling motor and seedling transplanting motor in real time with a sampling period of 100 ms. The remote controller synchronously transmits operation commands, such as travel control and transplanting operations, via the RS485 communication protocol. The aforementioned multi-source signals and commands are transmitted in real time to the system's main controller, providing the data foundation for subsequent coordinated computation.

During the main control processing and status display stage, the system's main controller, after receiving and parsing the multi-source signals, performs coordinated computation of the machine's operational logic and timing scheduling. The real-time speed feedback value of the traveling motor is multiplied by the preset dimensionless ratio coefficient K to serve as the target value for the PID control of the seedling transplanting motor speed, completing the core computation of speed-synchronized control. Simultaneously, operational status data—including real-time motor speeds, operation progress, and set planting spacing values—are transmitted to the OLED display via the IIC communication protocol, enabling real-time visualization of the machine's operating status.

Execution drive stage: The system's main controller outputs PWM speed regulation signals to the corresponding motor drivers, driving each actuator to complete the preset actions. The 24 V seedling transplanting motor driver controls the operation of the seedling transplanting motor, enabling gentle conveying of seedlings. The two 48 V traveling motor drivers independently control the two traveling motors, achieving traveling drive and differential steering control of the tracked chassis. Through closed-loop regulation using the speed-synchronized PID control algorithm, the real-time speed of the seedling transplanting motor continuously approaches the target speed, ultimately realizing precise matching between the chassis traveling speed and the seedling transplanting speed. This fundamentally ensures high consistency between the actual transplanting spacing and the preset value.

Straight-line deviation control is a key technical requirement in chassis design because it directly affects transplanting-row accuracy and helps prevent the machine from damaging the ridges or departing from the intended transplanting path. This study proposes a manual deviation-correction method based on a speed-correction coefficient. Straight-line travel is corrected by adjusting the rotational speeds of the left and right track motors.

The speed of a single track under the correction coefficient is calculated as follows:

$$\begin{cases} V_l = \dfrac{k_l n_1 \pi D(1\text{-}\delta)}{i_1 i_2} \\ V_r = \dfrac{k_r n_2 \pi D(1\text{-}\delta)}{i_1 i_2} \end{cases} \tag{9}$$

where:

V_l — corrected travel speed of the left track (m/min)

k_l — speed correction factor for left track motor (initial value = 1; manually adjustable via remote control) (dimensionless)

n_l — rotational speed of left brushless DC motor before correction factor compensation (r/min)

D — effective diameter of track driving wheel (0.15 m)

δ — total slip coefficient of transmission system, including chain elastic slip and track-ground slip (0.26)

i_1 — reduction gear ratio (60)

i_2 — sprocket-chain transmission ratio (0.79)

V_r — corrected travel speed of the right track (m/min)

k_r — speed correction factor for right track motor (default value = 1; manually adjustable via remote control) (dimensionless)

n_2 — rotational speed of right brushless DC motor before correction factor compensation (r/min)

The specific deviation correction control logic is as follows: the motor speed is determined by the duty cycle of the PWM signal output by the main controller, with the duty cycle being positively correlated with the motor speed. By multiplying the correction coefficient by the current duty cycle, precise adjustment of the motor speed is achieved, thereby altering the traveling speed of the single-side track. When the transplanter deviates to the right, the correction coefficients are adjusted to increase the speed of the right traveling motor and decrease the speed of the left traveling motor （k_r>1, k_l<1）, generating a leftward corrective torque that returns the machine to the preset straight trajectory. Conversely, the reverse adjustment strategy is applied for trajectory correction. This approach ultimately ensures the straight-line traveling accuracy of the whole machine, meeting the field operation requirements for *Panax notoginseng* seedling transplanting.

Test method

The overall stability of the *Panax notoginseng* transplanter is not only crucial for the safety of the remote operator and seedling feeders but also plays a key role in improving transplanting quality. In this study, the maximum roll angle is adopted to evaluate the stability of the whole machine on ridges and under longitudinal operating conditions *(Jiang et al., 2023)*.

Lateral Stability Analysis

Under no-load condition, the force diagram of the *Panax notoginseng* transplanter when stationary or moving straight at a uniform speed on a transverse slope is illustrated in Figure 6.

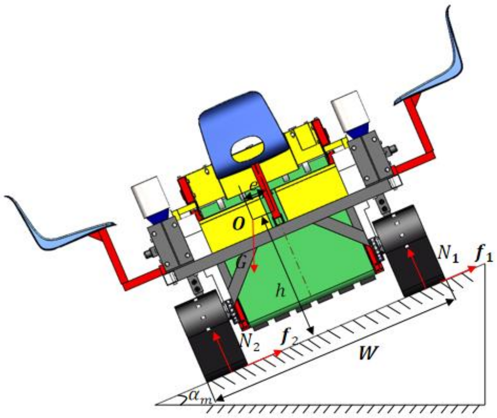

Fig. 6 - Schematic of lateral force analysis of crawler chassis for *Panax notoginseng* transplanter

The maximum roll angle α_m refers to the maximum slope angle at which the machine does not overturn when positioned on a transverse slope. According to the moment balance principle, when the machine is about to overturn about the edge of one track, the supporting force on that side becomes zero, and the moment of gravity about the pivot point is also zero.

Let the outer distance between the two tracks be W, the height of the center of mass be h, and the horizontal offset of the center of mass be e (positive to the left). The distances from the center of mass to the edges of the left and right tracks are then expressed as shown in Equation (10).

$$\begin{cases} L_L = \dfrac{W}{2} - e \\ L_R = \dfrac{W}{2} + e \end{cases} \tag{10}$$

where:

L_L — distance from mass center to the edge of left track (m)

L_R — distance from mass center to the edge of right track (m)

W — distance between outer edges of two tracks (m)

e — horizontal offset of mass center (m)

As shown in the figure, when the slope is inclined downward to the left, the critical condition for overturning about the left edge is as follows:

$$GL_L \cos\alpha_m = Gh\sin\alpha_m \tag{11}$$

The maximum roll angle formula can be derived as follows:

$$\alpha_m = \tan^{-1}\frac{\frac{W}{2}-e}{h} \tag{12}$$

If $W/2-e \leq 0$, the *Panax notoginseng* transplanter is already prone to overturning on level ground, and thus $\alpha_m=0$.

Based on theoretical calculations of relevant parameters for the *Panax notoginseng* transplanter and subsequent analysis using Equation (11), it can be determined that increasing the outer distance between the two tracks and lowering the height of the center of mass effectively enhances the lateral stability of the chassis. A larger maximum lateral roll angle α_m indicates superior lateral stability of the whole machine. Using the actual structural dimensions of the *Panax notoginseng* transplanter, the position of the center of mass was measured with SolidWorks software. The vertical distance from the center of mass to the ground was determined to be h=650 mm, the outer distance between the two tracks W=1360 mm, and the lateral offset of the center of mass relative to the longitudinal central plane e=150 mm. Substituting these parameters into the model yields a maximum lateral roll angle α_m=39.19° for the whole machine.

Ridging Stability Analysis

Deviation of the transplanter chassis or unevenness of the ridge may cause the tracks to ride onto the ridge slope, resulting in tilting of the transplanter and thereby increasing the risk of overturning. During *Panax notoginseng* transplanting operations, the ridge bottom width W_b is 850 mm, the ridge top width W_t is 720 mm, and the ridge height h ranges from 250 to 300 mm. The ridging state of the *Panax notoginseng* transplanter is illustrated in Figure 7.

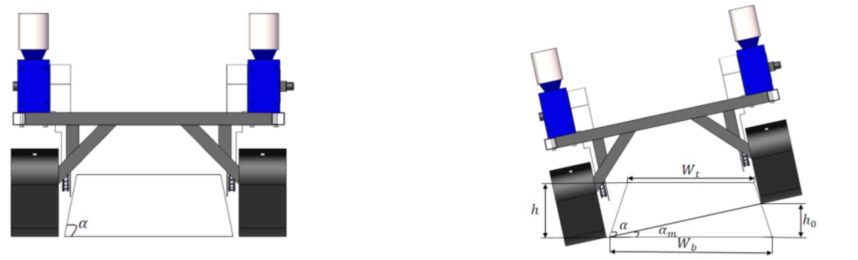

(a)Normal Ridge Alignment (b)Abnormal Ridge-Straddling State

Fig. 7 - Schematic of ridge-riding state of *Panax notoginseng* transplanter

$$\alpha = \tan^{-1}\frac{2h}{W_b - W_t} \tag{13}$$

$$\alpha_t = \tan^{-1}\frac{2hh_0}{2hW_b - h_0(W_b - W_t)} \tag{14}$$

where:

α — slope angle of ridge side (\(^\circ\))

h — ridge height (mm)

W_b — base width of ridge (mm)

W_t — top width of ridge (mm)

h_0 — vertical distance between the bottom of side track and ridge bottom under tilting state of transplanter (mm)

α_t — tipping angle (°)

Under the limit state where $h=h_0$, the inclination angle of the transplanter reaches its maximum operational value. Substituting $h=h_0$=300 mm, W_b=850 mm, and W_t=720 mm into the calculation yields α=77.8° and α_t=20.9°. This critical roll angle is smaller than the previously calculated maximum lateral roll angle α_m=39.19∘. Therefore, even if the transplanter unexpectedly rides onto the ridge surface, there is no risk of overturning.

Theoretical Calculation of Dynamic Performance

When operating in hilly and mountainous regions, the chassis must not only meet the requirements for lateral and ridge stability but also possess sufficient power reserve to handle extreme steep slope conditions reaching up to 25° or more in certain areas of Yunnan Province (*Guo et al., 2025*). Based on the parameters of the drive motor and transmission system outlined in Section 2.2, a theoretical verification of the maximum traction force and climbing capability of the chassis is conducted, providing performance expectations for subsequent field climbing tests.

The whole machine adopts a dual-motor synchronous drive configuration. After two stages of transmission, the maximum traction force of the chassis can be calculated using the following formula:

$$\begin{cases} T_0=\dfrac{9550P_0}{n_0} \\ F_{max}=\dfrac{2T_0 i_1 i_2 \eta}{r} \end{cases} \tag{15}$$

where: T_0 — rated torque of motor (N·m)

P_0 — rated power of motor (2.2 kW)

n_0 — rated rotational speed of motor (3000 r/min)

F_{max} — maximum traction force (N)

i_1 — transmission ratio of worm gear reducer (60)

i_2 — sprocket-chain transmission ratio (0.79)

η — total mechanical efficiency (0.85)

r — radius of driving wheel (0.075 m)

After calculation, the maximum traction force of the chassis is 7524 N, which meets the operational requirements of low-speed, high-load conditions.

Using the total resistance formula for slope traveling, the climbing capability under extreme operating conditions is verified for a design slope angle of 25°:

$$F_f=fG\cos\alpha+G\sin\alpha \tag{16}$$

where: F_f — maximum resistance force (N)

f — rolling resistance coefficient (0.15, dimensionless)

G — total gravity load (N)

α — slope inclination angle (25°)

The formula for the traction force reserve coefficient is given in Equation (17).

$$S=\frac{F_{max}}{F_f} \tag{17}$$

where: S — traction reserve coefficient (dimensionless)

F_{max} — maximum traction force of chassis (N)

F_f — maximum total running resistance on slope (N)

The total no-load mass of the whole machine is 780 kg, and the full-load mass is 1080 kg (including five operators). Calculations indicate that under full-load conditions, the maximum total resistance is approximately 5912 N, with a traction force reserve coefficient of about 1.27; under no-load conditions, the maximum total resistance is approximately 4270 N, with a traction force reserve coefficient of about 1.76. The traction force reserve is sufficient under all operating conditions, enabling stable adaptation to the steep slope requirements of ≥25° in the mountainous regions of Yunnan.

Steering Performance

Steering performance is a core indicator for the adaptability of the *Panax notoginseng* transplanter to narrow-row operations in mountainous areas, directly determining the machine's compatibility with complex terrain and its operational efficiency. This model adopts a pivot turning design, which fundamentally avoids issues such as damaging ridges or seedlings during turning. Therefore, the offset distance of the pivot turning center is selected as the key evaluation indicator for steering performance. During pivot turning of tracked vehicles in the field, longitudinal slip and lateral skid occur between the tracks and the ground due to soil characteristics, leading to deviations in the actual rotation center. Consequently, the calculation of the actual pivot turning center offset requires the introduction of correction terms for slip and skid. Based on the steering dynamics of tracked vehicles, the calculation formula (18) incorporating the effects of slip and skid is established.

$$R_{0,\delta}=\frac{Bk}{2(1-k)} \tag{18}$$

where: $R_{0,\delta}$ — actual offset of turning center under slipping turning condition (m)

B — track gauge of chassis (distance between centerlines of two tracks) (1.13 m)

k — steering slip coefficient (0.25, dimensionless)

Therefore, the theoretical offset distance of the pivot turning center during field operation is calculated to be 188 mm.

RESULTS AND ANALYSIS

Straight-line Traveling Speed Test

To verify the speed control accuracy of the traveling system and the reliability of the encoder speed measurement, and to provide data support for the coordinated matching between traveling speed and the seedling planting mechanism, a straight-line traveling speed test of the tracked chassis was conducted in accordance with GB/T 5668—2017, "Rotary Tillers"*(General Administration of Quality Supervision, Inspection and Quarantine of P.R.China & Standardization Administration of P.R.China, 2017)* .

The encoder is installed at the output shaft end of the traveling reducer, with a speed sampling period set to 100 ms. The output shaft speed is calculated by collecting the number of pulses per unit time, and the chassis traveling speed is estimated by combining transmission parameters, driving wheel dimensions, and slip rate correction. The speed measurement model is expressed as shown in Equation (19):

$$V_e=\frac{CN_0\pi D(1-\delta)}{Ni_2} \tag{19}$$

where: V_e — chassis travel speed calculated by encoder (m/min)

N_0 — encoder pulse count collected within 100 ms sampling period (1)

D — effective diameter of track driving wheel (0.15 m)

δ — total slip coefficient of transmission and travel system, including chain elastic slip and track-ground slip (0.26)

N — encoder resolution (10000 pulses per revolution)

i_2 — transmission ratio of sprocket-chain mechanism between reducer output shaft and driving wheel (0.79)

C — time conversion factor converting 100 ms sampling interval to minutes (600, dimensionless)

The test site was selected on a level and compacted field road surface within the Engineering Training Center of Kunming University of Science and Technology, with a road length of ≥30 m and longitudinal and transverse slopes of ≤1%, meeting the specifications for traveling performance testing of agricultural machinery.

During the test, the duty cycle of the PWM speed regulation signal for the traveling motor was set to 20%, 40%, 60%, 80%, and 100% via the remote controller, respectively, to control the whole machine to travel straight for 30 m at the corresponding set speeds. An electronic stopwatch was used to record the travel time for each pass. The test was repeated three times for each duty cycle parameter, and the arithmetic mean of the three measurements was taken to calculate the actual average traveling speed, which was then compared and analyzed with the speed synchronously measured by the encoder.

Table 2

Driving speed test results

Duty Cycle /%	Test No.	Time /s	Average Time /s	Actual Travel Speed (m/min)	Encoder-measured Travel Speed (m/min)
20	1	367.38	360.92	4.99	4.40
	2	357.36			
	3	358.02			
40	1	187.44	191.12	9.42	9.13
	2	197.22			
	3	188.7			
60	1	125.88	127.76	14.09	13.9
	2	127.50			
	3	129.90			

Duty Cycle /%	Test No.	Time /s	Average Time /s	Actual Travel Speed (m/min)	Encoder-measured Travel Speed (m/min)
80	1	97.38	96.06	18.74	17.85
	2	98.04			
	3	92.76			
100	1	83.92	83.47	21.56	21.32
	2	81.24			
	3	85.26			

The test results are presented in Table 2. The deviation between the encoder-measured speed and the actual average speed gradually decreases as the duty cycle increases. Under low-speed operating conditions, the deviation mainly arises from real-time fluctuations in track ground slip, elastic deformation of the transmission system, and differences in sampling scales between the long-stroke average speed and the short-period instantaneous speed. By calibrating and correcting the comprehensive slip rate coefficient, the encoder speed measurement can accurately approximate the actual traveling speed of the transplanter, thereby providing reliable data support for the coordinated speed control between traveling and seedling transplanting.

Straight-line deviation Test and Correction for the Transplanter During Traveling

The straight-line deviation test was conducted in accordance with the technical requirements and relevant test specifications for deviation under Clause 3.3.9 of the national standard GB/T 15370.4—2012, "Agricultural Tracked Tractors—Part 4: Technical Specifications for Belt Drive Tracked Tractors." The standard specifies that on a dry, hard, and level road surface with longitudinal and transverse slopes not exceeding 1%, the deviation of an agricultural tracked tractor over 100 m shall not exceed 6 m, which serves as the acceptance criterion for straight-line deviation *(General Administration of Quality Supervision, Inspection and Quarantine of P.R.China & Standardization Administration of P.R.China, 2012)*.

The straight-line deviation test of the transplanter was conducted by laying out a 30 m reference line in the test field, with marking points set every 5 m along the line. The initial position of the transplanter was aligned with the reference line, and the machine was driven at a uniform speed along the line. According to the aforementioned standard, the deviation over a 30 m travel distance shall not exceed 1.8 m, corresponding to a straight-line deviation of no more than 6%. The lateral deviation of the transplanter's traveling trajectory was measured using a tape measure. The field test setup for evaluating the straight-line deviation of the transplanter is shown in Figure 8.

Straight-line deviation is a core indicator for evaluating the degree of deviation, and its calculation expression is given as:

$$\gamma=\frac{max|y(x)-y_0(x)|}{L}\times 100\% \tag{20}$$

where: γ — straight-line deviation rate (%)

$y(x)$ — lateral coordinate of the actual travel path of the transplanter (dimensionless)

$y_0(x)$ — lateral coordinate of the ideal straight path, generally set to 0

L — straight-line test distance (30 m)

Fig. 8 - Straight-line travel deviation test of the transplanter

The straight-line traveling performance of the transplanter chassis directly determines the quality of ridged transplanting operations and the uniformity of plant distribution for *Panax notoginseng*. In this test, the straight-line deviation of the transplanter was measured under PWM duty cycles of 20%, 40%, 60%, 80%, and 100%, respectively. Through parameter calibration, the straight-line deviation was minimized as much as possible to enhance the precision and effectiveness of *Panax notoginseng* transplanting operations. The test results of the straight-line deviation before correction are shown in Table 3.

Table 3

Straight-line travel deviation of the transplanter before correction

Duty Cycle /%	Field Offset (Before Correction) /m			Mean straight-line deviation rate (Before Correction) /%
	Test 1	Test 2	Test 3	
20	1.63	1.67	1.72	5.58
40	2.23	1.92	2.13	6.98
60	2.16	2.09	2.2	7.17
80	2.06	2.45	2.36	7.63
100	2.48	2.39	2.56	8.26

As shown in the data in the table, the straight-line deviation of the transplanter gradually increases with the duty cycle, with most deviation values under each duty cycle exceeding the 6% limit specified in the national standard. If operated directly under such conditions, the transplanter would exhibit significant deviation during travel, leading to a high risk of the chassis riding onto the ridge. To avoid this problem, the remote operator would need to frequently apply minor steering corrections to maintain a stable travel path during operation. Therefore, this study introduces a straight-line deviation correction coefficient to address the issue of path deviation during transplanting operations. The straight-line deviation of the transplanter after correction is shown in Table 4, with the minimum value from three replicates used to determine the optimal correction coefficient.

Table 4

Straight-line travel deviation of the transplanter after correction

Duty Cycle /%	Lateral deviation after correction /m			Deviation rate corresponding to the minimum value /%
	Test 1	Test 2	Test 3	
20	0.32	0.26	0.29	0.87
40	0.34	0.24	0.28	0.8
60	0.45	0.38	0.25	0.83
80	0.78	0.43	0.32	1.07
100	0.32	0.47	0.36	1.07

Table 5

Correction coefficients of left and right motors under different duty cycles

Duty Cycle /%	Correction Parameters					
	Test 1		Test 2		Test 3	
	Right Motor	Left Motor	Right Motor	Left Motor	Right Motor	Left Motor
20	1	1.033	1	1.017	1	1.023
40	1	1.057	1	1.039	1	1.046
60	1	1.091	1	1.086	1	1.077
80	1	1.1	0.979	1.1	0.965	1.1
100	0.867	1.1	0.901	1.1	0.889	1.1

The correction coefficients for the left and right motors under different duty cycles are shown in Table 5. The test results indicate that the transplanter exhibits an overall leftward deviation when traveling on flat surfaces, which is attributed to the lower traveling speed of the left track compared to the right track. As the control duty cycle increases, the straight-line deviation of the whole machine tends to increase. To compensate for the speed difference between the two tracks and improve straight-line traveling accuracy, the correction coefficient for the left motor should be set greater than 1, while the correction coefficient for the right motor is either maintained at 1 or adjusted to less than 1.

The recommended correction coefficients for the left and right motors under different duty cycles are as follows: at 20% duty cycle, right motor 1, left motor 1.017; at 40% duty cycle, right motor 1, left motor 1.039; at 60% duty cycle, right motor 1, left motor 1.077; at 80% duty cycle, right motor 0.965, left motor 1.1; at 100% duty cycle, right motor 0.867, left motor 1.1.

Pivot Turning Center Offset Measurement

Steering performance is a core indicator of the field adaptability of tracked transplanters, directly determining the flexibility of inter-ridge turning and headland turning, as well as operational safety. This test was conducted in accordance with the steering performance test specifications for tracked tractors specified in GB/T 19040—2016, "Agricultural Tractors—Requirements for Steering" *(General Administration of Quality Supervision, Inspection and Quarantine of P.R.China & Standardization Administration of P.R.China, 2016)*. The pivot turning performance test of the transplanter was carried out on a typical soft field surface used for *Panax notoginseng* cultivation, where the track steering trajectory was measured and the turning center offset was determined.

(a) On-site turning test

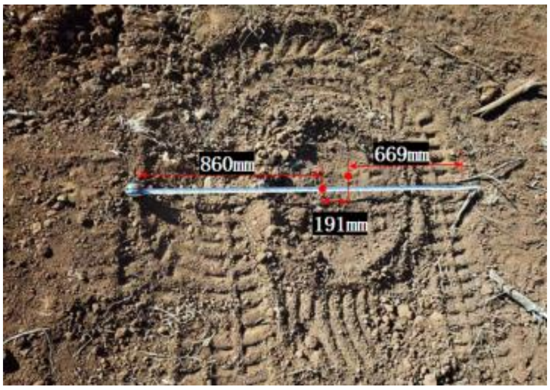

(b)Actual steering trajectory measurements

Fig. 9 - In-situ turning test of the transplanter

The test results indicate that the transplanter achieves stable pivot turning, with a measured turning center offset of approximately 191 mm, which is in close agreement with the previously calculated theoretical value. The turning accuracy and stability meet the operational requirements for *Panax notoginseng* transplanting in the field. The pivot turning test site and trajectory measurement results are shown in Figure 9.

Climbing Stability Test

In accordance with GB/T 3871.21—2015, "Agricultural Tractors—Test Procedures—Part 21: Stability" *(General Administration of Quality Supervision, Inspection and Quarantine of P.R.China & Standardization Administration of P.R.China, 2015)*, the climbing stability test of the *Panax notoginseng* transplanter was conducted. The test was performed on a slope with an inclination of 27°, and the machine was driven longitudinally and transversely on the slope at a travel speed of 10 m/min. The results showed that the transplanter successfully climbed the 27° slope during longitudinal travel and exhibited no instability or rollover during transverse travel on the 27° slope. The overall stability of the machine is excellent, meeting the operational requirements for ridged *Panax notoginseng* transplanting in the hilly and mountainous regions of Yunnan.

Fig.10 - Site of the vertical climb test

Fig.11 - Site of the lateral slope stability test

Ridged Traveling Stability Test

To verify the traveling stability of the transplanter under ridged slope conditions, a single-side ridge-crossing tilt travel test was conducted. One side of the transplanter's tracks was positioned to ride onto the ridge slope, and the machine was driven straight for 10 m along the ridge length at a uniform speed under different duty cycles. The traveling status of the whole machine was recorded, and no instability or overturning was observed throughout the process.

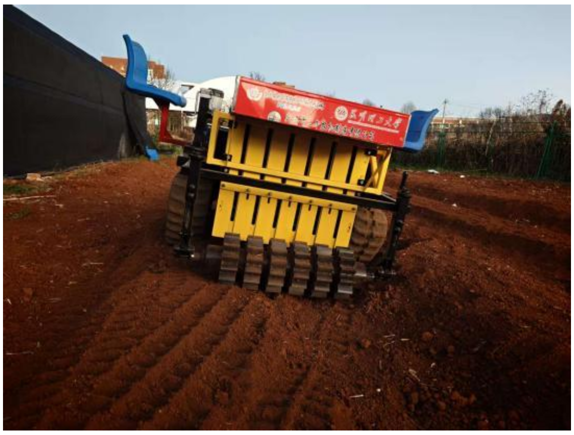

Fig.12 - On-ridge stability test

To verify the traveling stability of the transplanter under ridged slope conditions, a single-side ridge-crossing tilt travel test was conducted. The ridge parameters were fixed (ridge bottom width 850 mm, ridge top width 720 mm), and only the ridge height was varied to adjust the roll angle of the machine under different operating conditions. Three typical ridge heights for *Panax notoginseng* cultivation—200 mm, 250 mm, and 300 mm—were selected, corresponding to roll angles of 14.3°, 17.7°, and 20.9°, respectively, thereby establishing varying tilt operating conditions.

Table 6

Ridge-riding stability test results

Duty Cycle (%)	**Working Condition Lateral Tilt Angle (°)**		
	14.3	**17.7**	**20.9**
20	Pass	Pass	Pass
40	Pass	Pass	Pass
60	Pass	Pass	Pass
80	Pass	Pass	Pass
100	Pass	Pass	Pass

For each roll angle under different operating conditions, the transplanter was operated at five PWM speed regulation duty cycles of 20%, 40%, 60%, 80%, and 100%. The test was repeated three times for each condition, and the machine status was recorded. The test results are shown in Table 6. Under all combined conditions, the transplanter passed stably without overturning, verifying its traveling stability within this tilt range and across different operating parameters.

Motor Thermal Stability Test

Motor thermal stability is a core indicator determining the reliability of continuous field operation and the insulation service life of the transplanter's motors. In accordance with the mandatory requirements of Chapters 15 and 20 of GB/T 14711—2025, "General Requirements for Safety of Small and Medium-Sized Rotating Electrical Machines," concerning thermal testing and insulation structures, a thermal stability test was conducted on the variable-frequency speed-regulated brushless DC traveling motor with Class F insulation *(State Administration for Market Regulation & Standardization Administration of P.R.China, 2025)*. The test simulated load conditions of the transplanter under different operating speeds. The motor was operated continuously for 190 minutes under gradient PWM speed regulation duty cycles ranging from 20% to 90%, and the winding temperature was monitored in real time using a calibrated digital thermometer. Based on the heat resistance requirements for Class F insulation and accounting for a 20–30°C temperature margin between the motor housing and the winding, the evaluation criteria were established as follows: a safe operating range of 70°C to 90°C, and a forced shutdown protection threshold of 125°C to prevent insulation thermal aging.

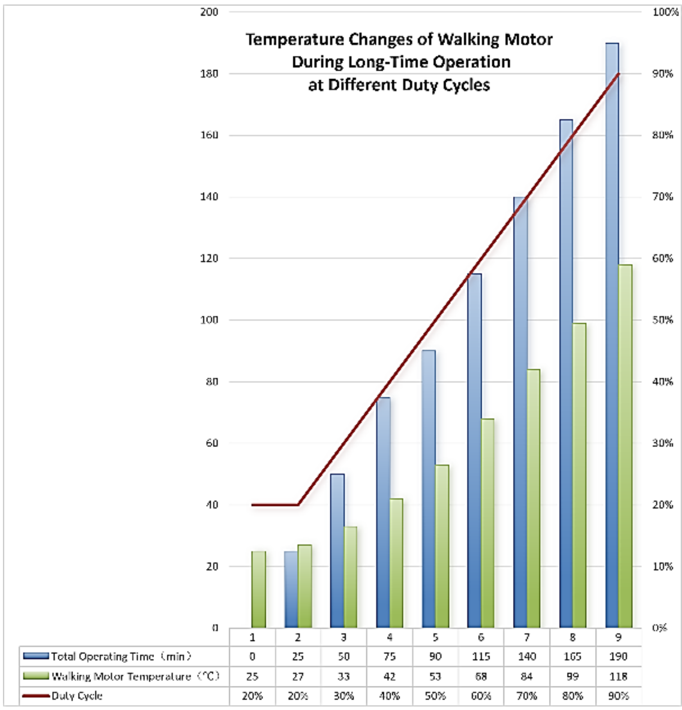

Fig.13 - Temperature change of driving motors under different duty cycle

The test results are shown in Figure 13: the motor temperature rise rate shows a clear positive correlation with the PWM duty cycle, consistent with the typical heating characteristics of small and medium-sized rotating electrical machines.

After 190 minutes of continuous operation, the final motor temperature reached 118°C, which did not reach the 125°C shutdown threshold, and remained within the safe operating range of 70°C to 90°C for most of the operation period. The test results meet the thermal safety requirements for continuous motor operation specified in GB/T 14711—2025, verifying that the traveling motor and transmission system possess good thermal stability and are capable of meeting the demands of prolonged continuous field operation for *Panax notoginseng* transplanting.

CONCLUSION AND DISCUSSION

An innovative design and theoretical modeling of a specialized tracked chassis for hilly and mountainous regions were completed. Addressing the complex agronomic requirements of ridged *Panax notoginseng* transplanting in Yunnan, the overall structure of a fully electric intelligent tracked chassis was designed. Based on the manual seedling feeding speed limit, a dimensionless ratio coefficient regulation model correlating planting spacing with traveling and seedling transplanting speeds was innovatively established. This enabled precise matching of the transmission ratio and theoretical calculation of the overall machine stability, laying the theoretical foundation for subsequent control system development.

A coordinated control system for traveling and seedling transplanting, along with a straight-line deviation correction scheme, was developed. A speed-synchronized PID control system based on speed-measuring encoders was designed to achieve real-time coordinated control between seedling conveying speed and chassis traveling speed. A manual deviation correction method utilizing a speed correction coefficient was proposed, effectively addressing the issue of traveling deviation in tracked chassis. Field tests demonstrated that, after correction, the straight-line deviation of the whole machine over a 30 m travel distance was controlled to within 1.1%, which is superior to the national standard limit.

The key performance indicators of the whole machine were verified to meet the operational requirements of hilly and mountainous regions. The chassis achieved a maximum traction force of 7524 N, a maximum climbing angle of ≥25°, and a maximum lateral roll angle of 39.19°, with the pivot turning center offset closely matching the theoretical value. Performance indicators including slope climbing stability, ridged traveling stability, and motor thermal stability all satisfied the requirements of relevant national standards. This chassis effectively enhances the automation level and operational accuracy of *Panax notoginseng* transplanting in hilly and mountainous regions, providing technical support for the intelligent upgrade of transplanting equipment for rhizomatous medicinal herbs.

ACKNOWLEDGEMENT

We would like to thank all colleagues for their advice and support throughout the research process.

REFERENCES

[1] Chen W.H., Li K.Z., Yang Y.F., Yang L., & Wang F. (2025). Design and experiment of a gantry-type electric crawler work vehicle (龙门式电动履带作业车设计与试验). *Forestry Machinery & Woodworking Equipment*, 53(12), 36-40. https://doi.org/10.13279/j.cnki.fmwe.2025.0154

[2] Dobretsov, R. Y., Sokolova, V. A., Teterina, I. A., et al. (2021). Interaction feature of caterpillar tracks with soil under significant axial displacements of pressure center. *IOP Conference Series: Earth and Environmental Science*, 839, 052023. https://doi.org/10.1088/1755-1315/839/5/052023

[3] General Administration of Quality Supervision, Inspection and Quarantine of P.R.China, & Standardization Administration of P.R.China. (2012). *General technical conditions for agricultural tractors Part 4: tracked tractors (GB/T 15370.4-2012)* (GB/T 15370.4-2012 农业拖拉机通用技术条件第4部分：履带拖拉机). China Standards Press, Beijing.

[4] General Administration of Quality Supervision, Inspection and Quarantine of P.R.China, & Standardization Administration of P.R.China. (2016). *Steering requirements for agricultural tractors (GB/T19040-2016)*(GB/T19040-2016 农业拖拉机转向要求). China Standards Press, Beijing.

[5] General Administration of Quality Supervision, Inspection and Quarantine of P.R.China, & Standardization Administration of P.R.China. (2015). *Agricultural tractor test code Part 21: stability (GB/T3871.21-2015)*(GB/T3871.21-2015 农业拖拉机试验规程第 21 部分：稳定性). China Standards Press, Beijing.

[6] General Administration of Quality Supervision, Inspection and Quarantine of P.R.China, & Standardization Administration of P.R.China. (2008). *General rules for determination of agricultural machinery test conditions (GB/T5262-2008)* (农业机械试验条件测定方法的一般规定:GB/T5262-2008). China Standards Press, Beijing.

[7] General Administration of Quality Supervision, Inspection and Quarantine of P.R.China, & Standardization Administration of P.R.China. (2017). *Rotary tiller (GB/T5668-2017)* (GB/T5668-2017 旋耕机). China Standards Press, Beijing.

[8] Guo G.Z., Jin G.Y., Luo Y.N., Luo H.T., Xie F.H., & He J.Y. (2025). Effects of slope on the service life of agricultural monorail surface (坡度对农用单轨轨面运行寿命的影响). *Transactions of the Chinese Society of Agricultural Engineering*, 41(15), 40–47. https://doi.org/10.11975/j.issn.1002-6819.202502045

[9] Han Z H, Zhu L C, Yuan Y W, et al. (2022). Passability analysis and optimal design of tracked chassis for mountain orchards on slope（山地果园履带底盘坡地通过性能分析与优化设计）. *Transactions of the*

Chinese Society for Agricultural Machinery, 53, 413–421, 448. https://doi.org/10.6041/j.issn.1000-1298.2022.05.045

[10] Hao J.J., Ai Q.H., Yuan D.C., Li Z.W., Yang S.H., & Zhao J.G. (2024). Design and experiment of electric self-propelled maize-peanut strip compound planting pesticide applicator (电动自走式玉米-花生带状复合种植模式施药机设计与试验). *Transactions of the Chinese Society for Agricultural Machinery*, 55(9), 216–225. https://doi.org/10.6041/j.issn.1000-1298.2024.09.018

[11] Jiang Y., Sun Z.Y., Wang R.C., Xia C.G., Ye Q., & Guo Y.F. (2023). Design and performance test of omnidirectional leveling system for crawler work machine in hilly areas（丘陵山区履带式作业机全向调平系统设计与性能试验）. *Transactions of the Chinese Society of Agricultural Engineering*, 39(18), 64-73. https://doi.org/10.11975/j.issn.1002-6819.202304190

[12] Li S.J., Peng J.B., Niu C.Q., Gao X.D., Qian Z.Y., Li M.Z., (2025), Design and Test of Articulated Steering Profiling Extended Range Wheeled Power Chassis for Hilly Orchards (丘陵果园铰接转向仿形增程轮式动力底盘设计与试验). *Transactions of the Chinese Society for Agricultural Machinery*, Vol.56, No.9, Wuhan/China, ISSN 1000-1298, pp.363-376, https://doi:10.6041/j.issn.1000-1298.2025.09.028

[13] Liu, C. K., Wang, L., & Meng, J. J. (2025). Theoretical analysis and empirical test of the impact of agricultural mechanization on agricultural ecological efficiency（农业机械化影响农业生态效率的理论分析及实证检验） *Chinese Journal of Eco-Agriculture*, 33, 1219–1234. https://doi.org/10.12357/cjea.20240202

[14] Liu H.Y., Zou S., Tang J.C., et al. (2025). Path tracking algorithm of tracked agricultural chassis based on parameter pre-adjusted super-twisting sliding mode control（基于参数预调型超螺旋滑模控制的履带农用底盘路径跟踪算法研究）. *Transactions of the Chinese Society for Agricultural Machinery*, 56, 136-144.https://doi.org/10.6041/j.issn.1000-1298.2025.02.013

[15] Liu Q., Ji Y.X., Yang F.Z., Zhang L.H., Du Z.X., Liu Z.J., & Zhu X.Y. (2025). Development and validation of traction performance prediction model for mountain tracked chassis on slopes (山地履带式底盘坡地牵引性能预测模型构建与试验). *Transactions of the Chinese Society for Agricultural Machinery*, 56(5), 597–607. https://doi.org/10.6041/j.issn.1000-1298.2025.05.058

[16] Mo F.Y. (2025). Design and optimization of chassis structure for tractors adapted to hilly and mountainous areas (丘陵山地适应性拖拉机底盘结构设计与优化). *Farm Machinery Using & Maintenance*, (11), 20-23.

[17] Mu X.D., Yang F.Z., Duan L.J., et al. (2024). Research status and development trend of key technologies of leveling and anti-overturn for hilly mountain tractors（丘陵山地拖拉机调平与防翻关键技术研究现状与发展趋势）. *Smart Agriculture*, 6, 1-16.

[18] Nie J.J., Xia K.T., Xie X.L., Lü Y.L., & Li C.M. (2025). Mobile chassis design and passability of arched waist agricultural robot（拱腰式农业机器人移动底盘设计与通过性研究）. *Transactions of the Chinese Society for Agricultural Machinery*, 56(10), 736-745. https://doi.org/10.6041/j.issn.1000-1298.2025.10.067

[19] Qi Z.Z., Zhou J., Ye Z.W., Zhou X.J., & Yang H.Y. (2024). Local path planning method in automatic walking of single-side brake steering track chassis（单侧制动式转向履带底盘自主行走局部路径规划方法）. *Transactions of the Chinese Society for Agricultural Machinery*, 55(6), 52-59. https://doi.org/10.6041/j.issn.1000-1298.2024.06.005

[20] Quan Q. & Ma S. (2010). Controllable postures of a dual-crawler-driven robot. *Mechatronics*, 20, 281-292. https://doi.org/10.1016/j.mechatronics.2010.01.001

[21] Rocha, F., Cid, A., Delunardo, M., et al. (2023). Body posture controller for actively articulated tracked vehicles moving over rough and unknown terrains. In 2023 *IEEE/RSJ International Conference on Intelligent Robots and Systems (IROS),* pp. 2330-2337. https://doi.org/10.1109/IROS55552.2023.10341528

[22] Shafae S.M., & Mousazadeh H. (2023). An operational scrutinization of autonomous tractor-trailer robot considering motion resistance force of rubber tracked undercarriage. *Cognitive Robotics*, 3, 173-184. https://doi.org/10.1016/j.cogr.2023.06.002

[23] State Administration for Market Regulation, & Standardization Administration of P.R. China. (2025). General safety requirements for small and medium rotating electrical machines (GB/T14711-2025) (中小型旋转电机通用安全要求:GB/T14711-2025) China Standards Press, Beijing.

[24] Wang P F, Yi J A, Zhu J X. (2025). Design and test of hydraulic system of power chassis for hilly and mountainous orchards (丘陵山地果园动力底盘液压系统设计与试验). *Transactions of the Chinese Society for Agricultural Machinery*, 56, 702–711, 722. https://doi.org/10.6041/j.issn.1000-1298.2025.06.066
[25] Xu L Y, Zhang J J, Yan X H. (2023). Review on electrification technology of agricultural equipment (农业装备电动化技术研究综述). *Transactions of the Chinese Society for Agricultural Machinery*, 54, 1–12. https://doi.org/10.6041/j.issn.1000-1298.2023.09.001
[26] Yu Q., Zhang X., Cao G., et al. (2025). Design and experiment of electric control system for self-propelled Chinese herbal materials transplanter. *Agriculture*, 15, 621. https://doi.org/10.3390/agriculture15060621
[27] Zhang X. (2025). *Design and test of precise transplanting control system for Panax notoginseng* (三七精准移栽控制系统设计与试验)[Master's thesis]. Kunming University of Science and Technology.
[28] Zhang X., Wang B.B., & Li M.T. (2025). Design and experiment of a multifunctional remote-controlled electric tracked chassis for hilly orchards in southern China (南方丘陵果园多功能遥控电动履带底盘设计与试验). *Modern Agricultural Equipment*, 46(6), 77-83. https://doi.org/10.3969/j.issn.1673-2154.2025.06.011
[29] Zhang Z.G., Deng Y.X., Wang F.A., Cao Q.Z., & Xie K.T. (2023). Trafficability analysis and scaling model experiment of self-propelled Panax notoginseng combine harvester chassis (自走式三七联合收获机底盘通过性能分析与模型试验). *Transactions of the Chinese Society for Agricultural Machinery*, 54(9), 164–177. https://doi.org/10.6041/j.issn.1000-1298.2023.09.016
[30] Zhao Z.Z., Zhang G.Z., Luo C.M., Liu W.R., Tang N.R., Kang Q.X., & Wang W.K. (2024). Path tracking algorithm of the dual motor tracked chassis considering skid and slip (考虑滑移滑转的双电机履带底盘路径跟踪算法). *Transactions of the Chinese Society of Agricultural Engineering*, 40(12), 46-54. https://doi.org/10.11975/j.issn.1002-6819.202401021
[31] Zhu L.C., Zhao Z.Y., Han Z.H., Wang R.X., Zhou L.M., & Zhao B. (2023). Design and experiment of dual-steering motion control system based on active disturbance rejection control (基于自抗扰控制的双重转向运动控制系统设计与试验). *Transactions of the Chinese Society for Agricultural Machinery*, 54(S1), 391–401. https://doi.org/10.6041/j.issn.1000-1298.2023.S1.042
[32] Zhu L.H. (2025). "Yuchai hybrid" accelerates the industrial reform of tractors (玉柴混动"加速拖拉机产业变革). *Agricultural Machinery Quality and Supervision*, (11), 40-41.